DESIGN OF A DYNAMIC OPTICAL PROPERTY MONITORING SYSTEM: STUDYING THE EFFECT OF TEMPERATURE CHANGE

by

ERCAN KARA

B.Sc., Electronics Engineering, Işık University, 2004

M.Sc., Biomedical Engineering, Boğaziçi University, 2008

Submitted to the Institute of Biomedical Engineering

in partial fulfillment of the requirements

for the degree of

Doctor

of

Philosophy

Boğaziçi University

2018

ACKNOWLEDGMENTS

First of all, I would like to express my sincere thanks to Prof. Dr. Murat Gülsoy for his support and motivation. He is a better advisor beyond my imagination. Despite the difficulties of working in another university, I would also thank to respond all my e-mails in 15 minutes to overcome it easily.

I am also grateful to Prof. Dr. İnci Çilesiz for sharing her experience and valuable guidance. I would like to thank Prof. Dr. Ata Akın for his ideas and support during the thesis progresses.

I would like to thank the rest of my thesis committee: Prof. Dr. Yasemin P. Kahya, Assoc. Prof. Dr. Özgür Kocatürk and Assist. Prof. Dr. Murat Tümer for their insightful comments and for allocating their time for critical reviewing of this thesis.

I would like to thank my friends Gamze Bölükbaşı Ateş and Özgür Kaya who helped me whenever I was stuck in the experiments. I would like to thank all the biophotonic family members, especially Nermin Topaloğlu Avşar, Ayşe Sena Kabaş Sarp, Hakan Solmaz and Burcu Tunç Çamlıbel for transforming the laboratory into a joyful place.

I wish to thank my dear wife Neriman who showed me patience and support in this process and my dear daughter Asya who always amazed me with her imagination.

ACADEMIC ETHICS AND INTEGRITY STATEMENT

I, Ercan Kara, hereby certify that I am aware of the Academic Ethics and Integrity Policy issued by the Council of Higher Education (YÖK) and I fully acknowledge all the consequences due to its violation by plagiarism or any other way.

Name :

Signature:

Date:

ABSTRACT

DESIGN OF A DYNAMIC OPTICAL PROPERTY MONITORING SYSTEM: STUDYING THE EFFECT OF TEMPERATURE CHANGE

In laser applications, it is necessary to know the tissue optical properties before the treatment and how they change during the treatment. The optical monitoring system with double-integrating-sphere having a special sample heating apparatus was designed to investigate the effect of temperature on optical properties. Temperature dependent optical property changes was investigated using lipid emulsion. It was found that the reflectance value showed negative correlation with temperature and transmittance showed positive correlation. Also, it was observed that the reduced scattering coefficient obtained using an inverse adding-doubling method showed a negative correlation with temperature, but there was no statistically significant change in absorption coefficient. The effect of such optical property changes on the light propagation was displayed by Monte Carlo simulation. As a result, optical properties can change with temperature and this change must be taken into account for safer laser applications.

Keywords: Double-Integrating-Sphere, Temperature Effect, Optical Property, Monte Carlo Simulation.

ÖZET

DİNAMİK OPTİK ÖZELLİK İZLEME SİSTEMİNİN TASARIMI: SICAKLIK DEĞİŞİM ETKİSİNİN İNCELENMESİ

Lazer uygulamalarında, tedaviden önce ve tedavi sırasında dokunun optik özelliklerinin nasıl değiştiklerini bilmek gereklidir. Sıcaklığın optik özelliklere etkisini araştırmak için özel bir ısıtma aparatına sahip çift-toplayıcı-küreli optik izleme sistemi tasarlandı. Lipid emulsiyonu kullanılarak, sıcaklığa bağlı optik özelliklerin değişimi incelendi. Sıcaklık ile yansımanın negatif, geçirgenliğin pozitif bir korelasyon gösterdiği bulundu. Ayrıca, IAD yöntemi kullanılarak elde edilen indirgenmiş saçılma katsayısının sıcaklık ile negatif korelasyon gösterdiği fakat soğurma katsayısında istatistiksel olarak anlamlı bir değişim olmadığı gözlemlendi. Optik özelliklerdeki bu değişimlerin ışık yayılımı üzerine etkisi Monte Carlo simülasyonu ile gösterildi. Sonuç olarak, sıcaklıkla optik özellikler değişebilir ve daha güvenli lazer uygulamaları için bu değişim dikkate alınmalıdır.

Anahtar Sözcükler: Çift-Toplayıcı-Küre, Sıcaklık Etkisi, Optik Özellik, Monte Carlo simülasyonu. .

TABLE OF CONTENTS

LIST OF FIGURES

LIST OF TABLES

LIST OF SYMBOLS

g	Anisotropy Factor
M_R	Normalized Reflectance
M_T	Normalized Transmittance
R	The Detector of the Reflectance sphere
T	The Detector of the Transmittance sphere
μ_a	Absorption Coefficient
μ_s	Scattering Coefficient
$\mu_s{}'$	Reduced Scattering Coefficient

LIST OF ABBREVIATIONS

DAQ	Data Acquisition
IAD	Inverse Adding Doubling
MOSFET	Metal-Oxide-Semiconductor Field Effect Transistor
NI	National Instruments
NIRS	Near Infrared Spectrum
RTE	Radiative Transport Equation
UV	Ultra Violet
VIS	Visible Spectrum

1. INTRODUCTION

Lasers are widely used in many medical applications, including dermatology, ophthalmology, cardiology, etc. They can be used for diagnostic and therapeutic purposes. It is important to observe the behavior of tissue without any damage in diagnostic applications whereas the only specific region of the tissue should be affected in therapeutic applications such as removing of cancer tissue with laser. Better understanding of laser tissue interaction mechanisms requires to study on the optical properties of biological tissues since these properties are prominent factors to determine the temporal and spatial distribution of light within the tissue [1, 2].

Also, the thermal damage and its effects on tissue should be taken into consideration in laser treatment. Heat generation and resultant thermal damage is determined largely by absorption coefficient during the laser treatment. When photons are absorbed by a tissue, the light energy is transformed into thermal energy and heat transfer starts. Thermal damage can progress from denaturation and coagulation to ablation [3].

The effect of temperature induced by laser in the tissue is necessary for accurate and safe treatment. The optical characteristics of tissues and their dynamic behavior during the treatment should be well known to keep the temperature under control and make the treatment safer. Temperature field is not only dependent on laser parameters such as wavelength, power density, beam size, laser mode, and exposure time but also dependent on the optical properties of tissues, namely absorption coefficient μ_a, scattering coefficient μ_s, and anisotropy factor g. These parameters determine the temporal and spatial light distribution within the tissue and thereby the temperature induced optical property changes should be determined [1, 2].

Optical properties are generally determined by indirect methods in room temperature. Obtained optical properties are used to define the light propagation within

the tissue under the assumption that they do not change during the laser treatment. However, microscopic and macroscopic changes occur during the laser treatment [2]. These changes alter the structure and composition of the tissue and result in the changes in optical properties. Therefore, optical properties are the necessary parameters for an accurate planning of laser therapy where the optical properties exhibit a dynamic change during the treatment.

Optical properties of tissues play an important role in laser diagnosis and treatments. One should know the behavior of tissue optical properties to plan a safer treatment. Because they are the main factors to affect the light propagation within the tissue.

1.1 Optical Properties of Tissues

1.1.1 Refraction Index

The ratio of the velocity of the light in the vacuum to the velocity of the light in the medium is called the refraction index and is calculated as follows

$$n = \frac{c}{v} \tag{1.1}$$

where c and v represent the speed of light in ambient and vacuum, respectively. c equals to 299,792,458 m/s. In addition, the refractive index varies with wavelength and it is responsible for the reflection and refraction rates of the light applied on a tissue.

1.1.2 Reflection, Refraction and Transmittance

Reflection is the light reflected from the surface between two different media having different refraction indexes (Figure 1.1). If the irregularities on the surface are

negligible compared to the wavelength, this reflection is called specular reflection. However, when these irregularities are in the order of wavelength or larger, the phenomenon called diffuse reflection comes into play. In almost all tissues, diffuse reflection occurs due to roughness on the surface. Reflectance is the ratio of the reflected light intensity to the incident light intensity.

Refraction appears as a change in direction of light when it is passing through a media having a different refractive index. It is caused by the difference in the speed of light. The refraction angle can be calculated by the Snell law.

$$\frac{sin\theta_1}{sin\theta_2} = \frac{v_1}{v_2} = \frac{n_2}{n_1} \tag{1.2}$$

where θ_1 and θ_2 are the angles of incident and refracted light, v_1 and v_2 are the velocities at the first and second medium, and n_1 and n_2 are the refractive indices of the first and second medium, respectively.

If no light is transmitted and all the light is reflected, this is called total internal reflection. Also, if no light is reflected, the angle of that case is called Brewster's angle.

Only the photons scattered in the forward direction from the refraction wave pass to the other side of slab and form the transmitted light. The ratio of transmitted light intensity to the initial light intensity is called transmittance.

1.1.3 Absorption

Absorption is defined as the attenuation of the electromagnetic wave when it passes through the medium. It is a wavelength dependent. The medium is called opaque when no transmission occurs. The transparent medium allows the transmission of all light without absorption. The absorption coefficient is the probability of photon absorbed per unit length.

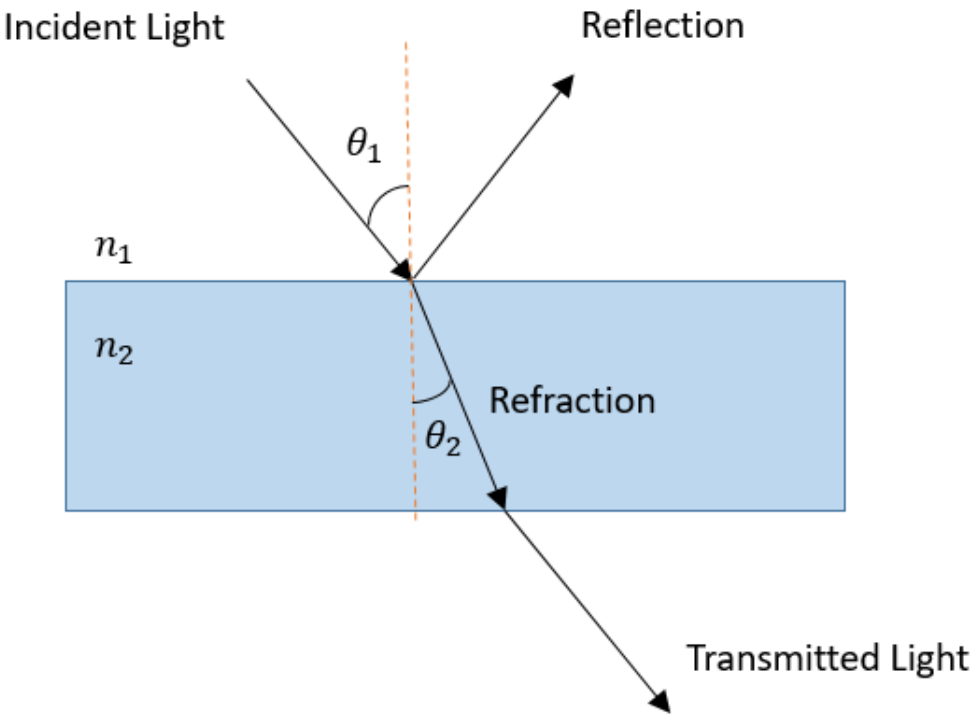

Figure 1.1 Illustration of reflection, refraction and transmission

1.1.4 Scattering

Scattering can be analyzed as an elastic and inelastic scattering. In the inelastic scattering, such as Brillouin and Raman, the energy of the scattered photon changes. However, the energy of photon remains the same after scattering in the elastic scattering. It is caused by the refraction index changes due to the inhomogeneities in the tissue. Whereas Rayleigh type of elastic scattering results from that the size of inhomogeneities is smaller than the wavelength, Mie scattering occurs when the particle size is in the order of the wavelength. Also, the scattering coefficient is defined as the probability of photon scattered per unit length.

1.1.5 Anisotropy Factor

Anisotropy factor is the average cosine of scattering angles. It is denoted by g and can be calculated as

$$g = \frac{\int_{4\pi} p(\theta) cos\theta d\omega}{\int_{4\pi} cos\theta d\omega} \tag{1.3}$$

where $p(\theta)$ is the probability function of a scattered photon with the angle of θ. It can take values from -1 to 1. While the positive values of g define the forward scattering, the negative values express the back scattering.

The reduced scattering coefficient is defined as

$$\mu_s^{'} = (1 - g)\mu_s \tag{1.4}$$

1.1.6 Turbid Media

The media in which both scattering and absorption occur is called turbid media. Optical albedo of this media is defined as:

$$a = \frac{\mu_s}{\mu_s + \mu_a} \tag{1.5}$$

1.2 Determination of Optical Properties

Methods for obtaining the optical properties of tissue are divided into two groups: the approximate analytic solutions and the numerical solutions of Radiative Transport Equation (RTE)[1, 3]. Analytic solutions which are also called non-iterative solutions are based on the solution of RTE under some assumptions because of the complexity of the solution. For example, Beer's law or first order scattering is applicable only to very thin tissue slabs and ignores the multiple scattering. Therefore, this method is appropriate only for thin tissue samples having low scattering coefficient. Another direct method is the Kubelka-Munk approach used when but it suffers from accuracy. Diffusion approximation which contains time-resolved spectroscopy and radial reflectance spectroscopy has a poor approximation when optical albedo is close to 0.5. One of the most used numerical or iterative approach is Monte Carlo Method. It is based on a random walk of photon propagation within the tissue. It has a good accuracy if the number of photons is large but it suffers from the computational time. The other iterative technique is based on integrating sphere and inverse adding doubling which will be explained in the next section.

1.3 Double Integrating Sphere Technique

Integrating spheres are used to measure the transmittance and reflectance. They are coated with highly reflective materials. LabSphere 4P-GPS-033-SL model integrating spheres were used in this study. The internal walls of the spheres are coated with

Spectralon which is highly flat characteristics in the Ultraviolet (UV), Visible Spectrum (VIS)and Near Infrared Spectrum (NIRS). It also shows a close response to Lambertian behavior. When the light comes into integrating sphere, it starts to reflect from the walls of integrating sphere and the detector measures the light intensity.

In order to perform simultaneous measurements of transmittance and reflectance, double-integrating-sphere technique is used. The main advantage of this technique is that the measurements can be performed at the same time. In this technique, sample is placed between two integrating spheres and diffuse reflectance and total transmittance measurements could be performed. Total transmittance includes diffuse transmittance and collimated transmittance. Also, the total reflectance is equal to diffuse reflectance and specular reflectance. Moreover, the value of μ_a and the value of the reduced scattering coeffcient $\mu_s^{'} = \mu_s(1-g)$ could be calculated from the measurements which will be explained in the next section. If the value of g is need to be calculated, collimated transmittance should be to be measured. Collimated transmittance could be measured by placing a third detector to the second integrating sphere exit port.

1.4 Inverse Adding Doubling Method

Inverse Adding Doubling (IAD) developed by Prahl et al. is a method to obtain scattering and absorption coefficient from the transmittance and reflectance measurements [4]. It is fast and has a good balance between speed and accuracy. The inverse in the name of IAD refers to the reversal process of calculating the transmittance and reflectance from optical properties. Doubling method depends on that if the reflection and transmission of a thin slab of tissue at a certain angle is known, total reflection and transmission of the same tissue which is twice in thickness can be calculated by adding the contributions of two thin layers. Thus, the total reflection and transmission of a tissue sample can be calculated by doubling the thickness of a thin slab tissue whose optical properties are known until reaching the desired thickness. The adding refers to the doubling of different tissue slabs and provides to calculate optical properties of layered tissues with different optical properties[1].

IAD is an iterative method which includes the following steps:

- Defining the below sample geometry and sphere parameters:
  - Thickness of sample
  - Thickness of slides
  - Diameter of illumination beam
  - Reflectance of Calibration Standard
  - Number of Spheres
  - Reflection and Transmission Sphere Diameters
  - Reflection and Transmission Sphere Sample Port Diameters
  - Reflection and Transmission Sphere Entrance Port Diameters
  - Reflection and Transmission Sphere Detector Port Diameters
  - Reflectivity of the sphere walls
  - Index of refraction of sample
  - Index of refraction of slides
- Calculation of the reflections and transmissions
- Comparison of calculated and measured reflectance and transmittance
- Repeating the same procedure until the estimated value converges to measured value with a desired accuracy

One of the problems should be considered when taking a measurement with a double-integrating-sphere is the light loss coming out of the sample edges. This error can result in an overestimation of absorption coefficient. This problem was solved by adding a Monte Carlo code to IAD to predict the light loss effect. Another problem which is the non-linear effect of the integrating sphere also solved in IAD [5].

In this study, the value of μ_a and the value of $\mu_s^{'}$ were estimated by using a double-integrating-sphere technique. The optical measurements were performed by

irradiating the sample between integrating spheres. The diffuse reflectance is measured in the first integrating sphere by collecting the reflected and back-scattered light while the total transmittance is measured in the second sphere by integrating the transmitted and forward scattered light.

The measured reflectance and transmittance values are not directly used in IAD program. The measured values should be normalized with the incident light[6]. The normalized reflectance M_R is calculated as

$$M_R = r_{std}.\frac{(R_2(r_s^{direct}, r_s, t_s^{direct}, t_s) - R_2(0,0,0,0))}{(R_2(r_{std}, r_{std}, 0, 0) - R_2(0,0,0,0))} \tag{1.6}$$

and the normalized transmittance M_T is calculated as

$$M_T = \frac{(T_2(r_s^{direct}, r_s, t_s^{direct}, t_s) - T_2(0,0,0,0))}{(T_2(0,0,1,1) - T_2(0,0,0,0))} \tag{1.7}$$

where r_{std} is the value of the reflectance standard, $R_2(r_s^{direct}, r_s, t_s^{direct}, t_s)$ is the diffuse reflectance measurement with the sample, $R_2(0,0,0,0)$ is the background noise of the reflectance sphere, $R_2(r_{std}, r_{std}, 0, 0)$ is the maximum diffuse reflectance value with the reflectance standart, $T_2(r_s^{direct}, r_s, t_s^{direct}, t_s)$ is the total transmittance measurement, $T_2(0,0,1,1)$ is the maximum transmittance value and $T_2(0,0,0,0)$ is the background noise of the transmittance sphere with the sample. The necessary measurements to calculate M_R and M_T are shown in Figure 1.2

1.5 Dynamic Optical Property Measurements with Integrating Sphere Technique

Temperature related optical property measurements suffer from insufficient experimental setup. In most of the studies, tissue is thrown into hot water bath before the measurements and then the measurements are taken in room temperature. This system avoids to investigate the temperature dependent optical property changes. It only helps to find the thermal damage effects on optical properties.

The studies having a double-integrating-sphere setup to measure the direct relationship between optical properties and temperature are limited.

Agah et al. designed a two-port plastic tissue holder which was connected to a water bath [7]. The tissue was heated by pumping a heated saline to the tissue holder. They observed that the reduced scattering coefficient increased and absorption increased with temperature.

Laufer et al. performed the optical measurements in neonatal incubator to study the temperature dependence of optical properties of human dermis and subdermis [8]. The measurements were performed from 25°C to 40°C. They found that the normalized scattering coefficient increased for dermis and decreased for subdermis as the temperature increased. A significant difference in absorption coefficient could not be found for both tissue samples.

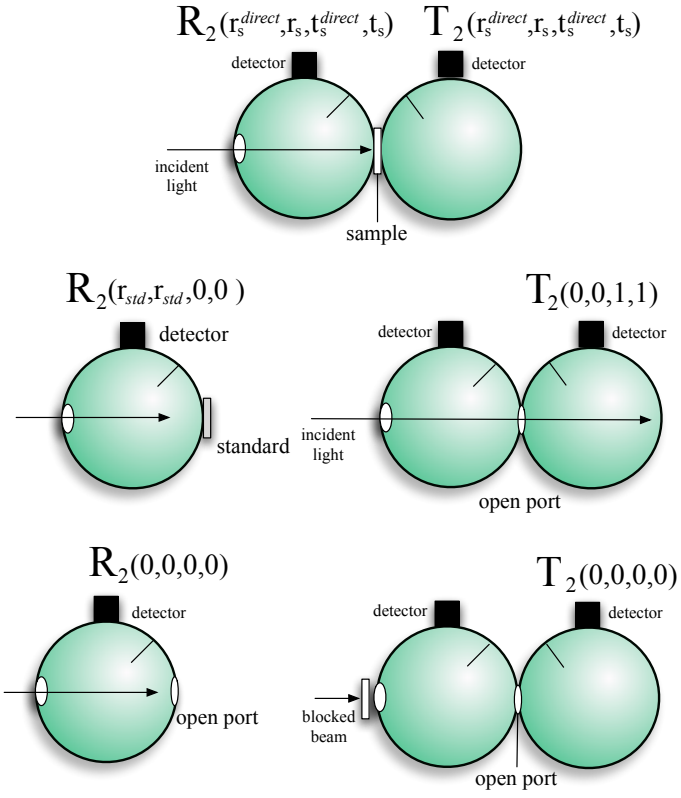

Figure 1.2 Measurements needed for M_R and M_T when two integrating spheres are used (Image taken from IAD manual).

Skinner et al. designed a metallic sample holder system to measure the optical property changes of ex vivo rat prostate due to heating [9]. The sample was heated by circulating constant temperature water through the sample holder. They found that the reduced scattering and absorption was altered.

Basu et al. created a sample holder by sandwiching cartilage tissues between aluminum plates [10]. Then, tissue was heated by hotplate by using single sphere. They found that diffusely transmitted light decreased, then stayed almost constant and increased during temperature increase. However, diffusely reflected light showed an opposite trend.

Soogeun et al. studied the effect of temperature dependent changes on the fluence rate [11]. They took the measurements inside the styrofoam box whose temperature was adjusted by heating gun. They observed that the reduced scattering coefficient decreased when temperature increased from 25°C to 40°C.

If tissues are subjected to high temperatures, its physical and optical properties can alter. Therefore, there is a need for the study to investigate how the optical properties due to temperature change.

The aim of the thesis is to develop a new temperature adjustable optical measurement system and to investigate how the optical properties of lipid emulsion change with the temperature.

2. SYSTEM DESIGN

The system design is based on double-integrating-sphere technique. A new temperature adjustable optical measurement with double-integrating-sphere was designed to explore the effects of temperature on the optical properties of samples.

Temperature-dependent optical measurements were performed using the designed system shown in Figure 2.1. It has an ability to perform sequential reflectance and transmittance measurements. A 635-nm diode laser (VA-I-400-635, Optotronics, USA) was used as the light source. The beam focused on the sample and its size reduced to 2.3 mm by using lenses and diaphragms. A double-integrating sphere (4P-GPS-033-SL, LabSphere) was used to measure the reflected and transmitted light detected by silicon detectors denoted as R and T (SDA-050-P-RTA-CX, Lab-Sphere), respectively. Reflectance and transmittance measurements were performed sequentially at 5 s intervals. Port sizes were adjusted by adaptors. Chopper (SR540, Stanford Research Systems) and lock-in amplifiers (SR510, Stanford Research Systems) were used to eliminate the background noise by modulating the incoming light and to extract the detected modulated signals coming from the detectors.

In order to measure the temperature dependence of transmittance and reflectance, a new sample holder and a control unit was designed and LabVIEW based user interface program was prepared.

2.1 Sample Holder Design

The cuvette shown in Figure 2.2 was designed to take measurements from the liquid samples. First, a frame was formed by cutting acrylic plate. Then, the cuvette was constructed by gluing the coverslips to acrylic frame. Two ports were opened for lipid injection and temperature sensor insertion. The cuvette was sandwiched between

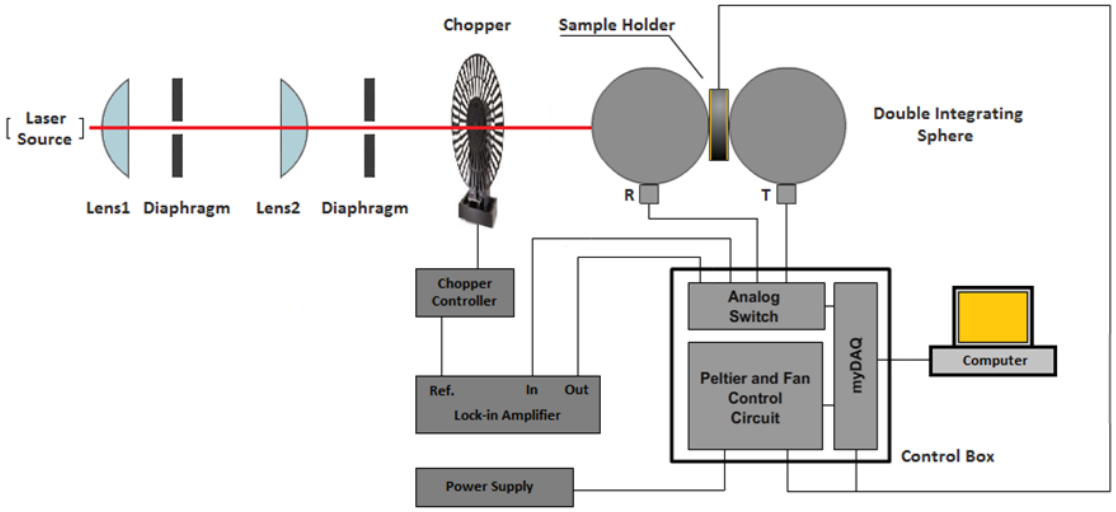

Figure 2.1 Experimental setup.

Figure 2.2 Sample cuvette with temperature sensor.

two copper plates and the peltier modules (TEC1-4905, 4.5V, 17W, 25x25 mm) were added to control the temperature as shown in Figure 2.3, Figure 2.4 and Figure 2.5. Fans also included to increase the efficiency of the peltier modules.

2.2 Control Unit

Control unit is consisted of a data acquisition (DAQ) device, a bilateral analog switch and temperature control circuit. National Instruments (NI) myDAQ was used as a DAQ device. It is a compact data acquisition device has two analog inputs, two analog outputs and eight digital input and outputs. It can also be combined with NI LabVIEW program to control and analyze the signals.

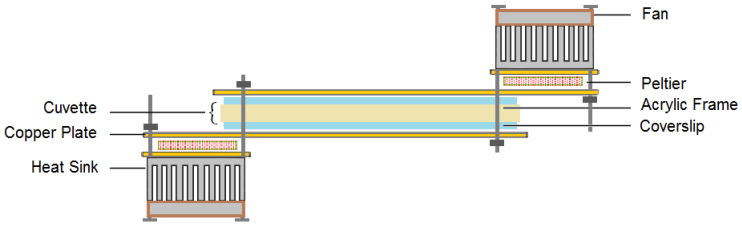

Figure 2.3 Top view drawing of the sample holder.

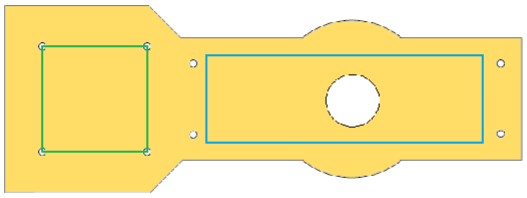

Figure 2.4 Front view drawing of the sample holder.

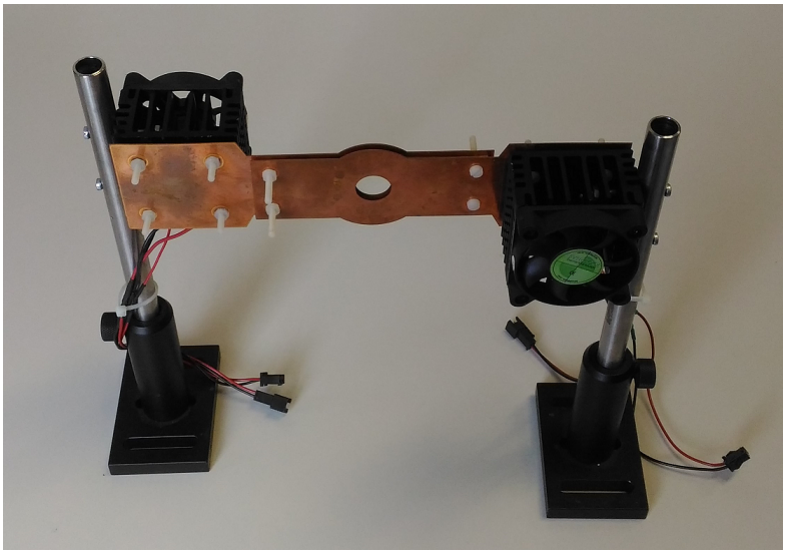

Figure 2.5 The picture of sample holder.

The light come from the source enters the first integrating sphere and reaches the sample placed between the double integrating spheres. Then, the light is reflected from the sample, absorbed by the sample and passes through the sample. The reflected light intensity is measured by the first detector denoted by R and the transmitted portion is measured by the second detector denoted by T (Figure 2.1). However, the detectors have no wavelength selectivity and operate in a certain wavelength range. In this study, silicon detectors (SDA-050-P-RTA-CX, Lab-Sphere) were used. They can operate in visible spectrum (380-780nm). Therefore, it should be eliminated the effect of wavelengths other than the applied one against the possibility of entering light into the spheres from another source. Lock-in amplifier and chopper duo are well suited for this job. The chopper is a device which blocks the incoming light periodically. The period or the frequency is controlled by the chopper controller. Lock-in amplifier is a device which is used to extract the signal embedded in a noisy environment. It has a reference input, signal input and output. It recovers the amount of useful signal in the input signal modulated by the reference signal.

In the experimental setup, there is only one lock-in amplifier. Therefore, a bidirectional analog switch of 74HC4066 was used to switch the signals coming from the R and T detectors sequentially. Hence, it gives us to opportunity to measure the reflectance and transmittance with 5 sec intervals.

2.2.1 Temperature Control Circuits

H-bridge is generally used in servo motor control. In this project, it was used as a Peltier control circuit. The operation principle is shown in Figure 2.6. ON/OFF switch is used to turn on or off the heater and cooler mechanism. When it is ON state and H1 and H2 switches are closed, the peltier starts to heat up the tissue. When C1 and C2 switches are closed, the polarity of voltage and the direction of the current flowing through the peltier will be reversed and it will cool down the tissue.

In the first version of the circuit, the switch function was implemented by

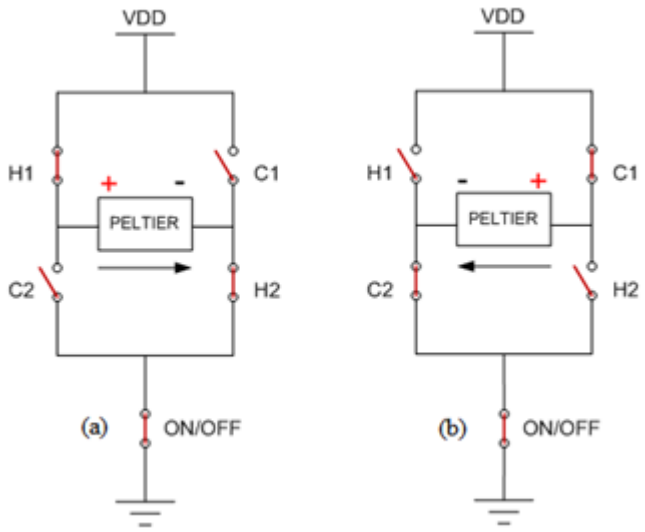

Figure 2.6 H-bridge circuit as a heater (a) and a cooler (b).

IRF530 N-channel power Metal-Oxide-Semiconductor Field Effect Transistors (MOSFETs) considering the high current drawn by Peltier (Figure 2.7). Optocoupler (4N26) isolates DAQ and power supply parts to prevent any damage. It consists of LED and phototransistor. When no voltage is applied to the input of R1 resistor, no current flows through the LED, the phototransistor is in cut-off region. So, no current flows the R2 resistor. Gate-source voltage of N-MOS transistor is equal to zero and the M1 transistor is in cut-off region. In short, if the input of the circuit is 0, MOS transistor will act as an open switch. However, if a positive voltage is applied to R1 resistor, LED emits a NIR light and the light falls upon the base of the transistor makes the phototransistor conducting and there will be a positive voltage across R2 resistor. This enables MOS transistor to act as a closed switch. The schematic of the H-bridge circuit is shown in Figure 2.8. While M3 transistor acts as an ON-OFF switch, M1-M5 and M2-M4 couples act as a heating and cooling switches, respectively.

The P-Spice simulation of this circuit is shown in 2.9. There are three digital input voltages denoted by ON-OFF, H-C and PWM as shown at the top of the graph. R11 symbolizes the Peltier. Therefore, the signal at the bottom symbolizes the current flowing through the Peltier. When the ON-OFF signal is at low level, the current passing through R11 resistor is zero. When it is ON state, the direction of the current changes with the state of H-C signal and it is modulated by PWM signal.

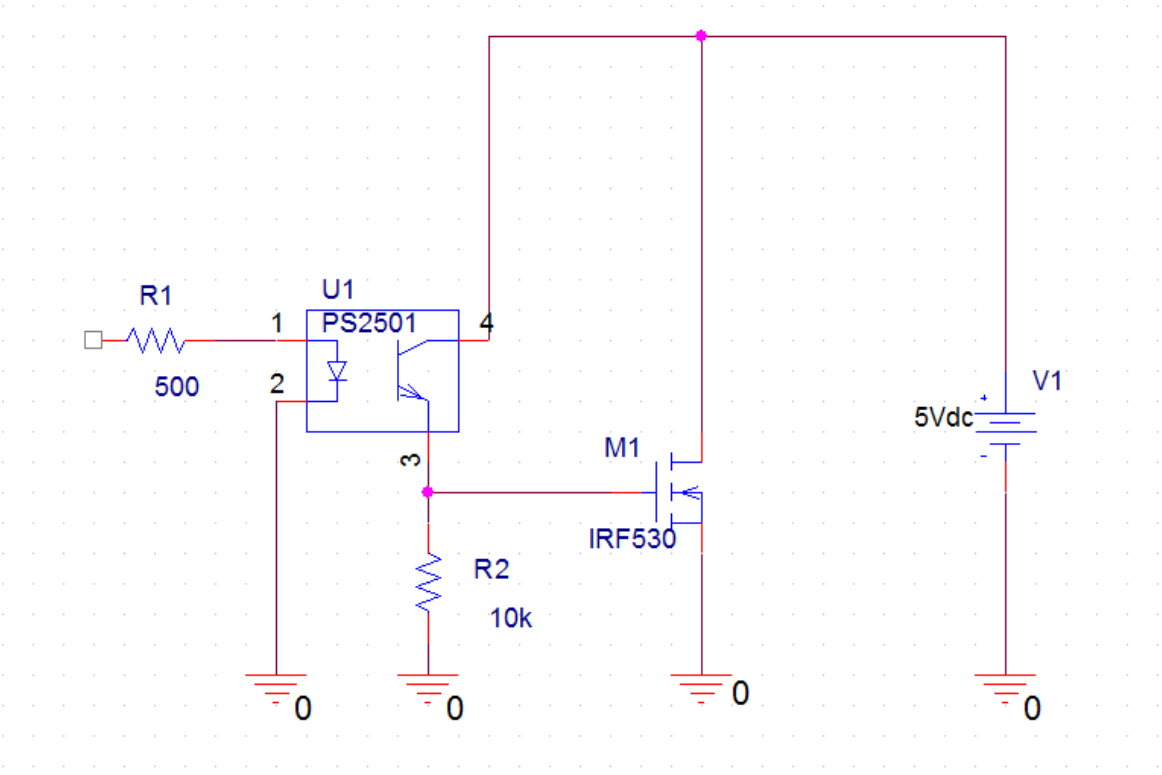

Figure 2.7 N-channel MOS as a switch.

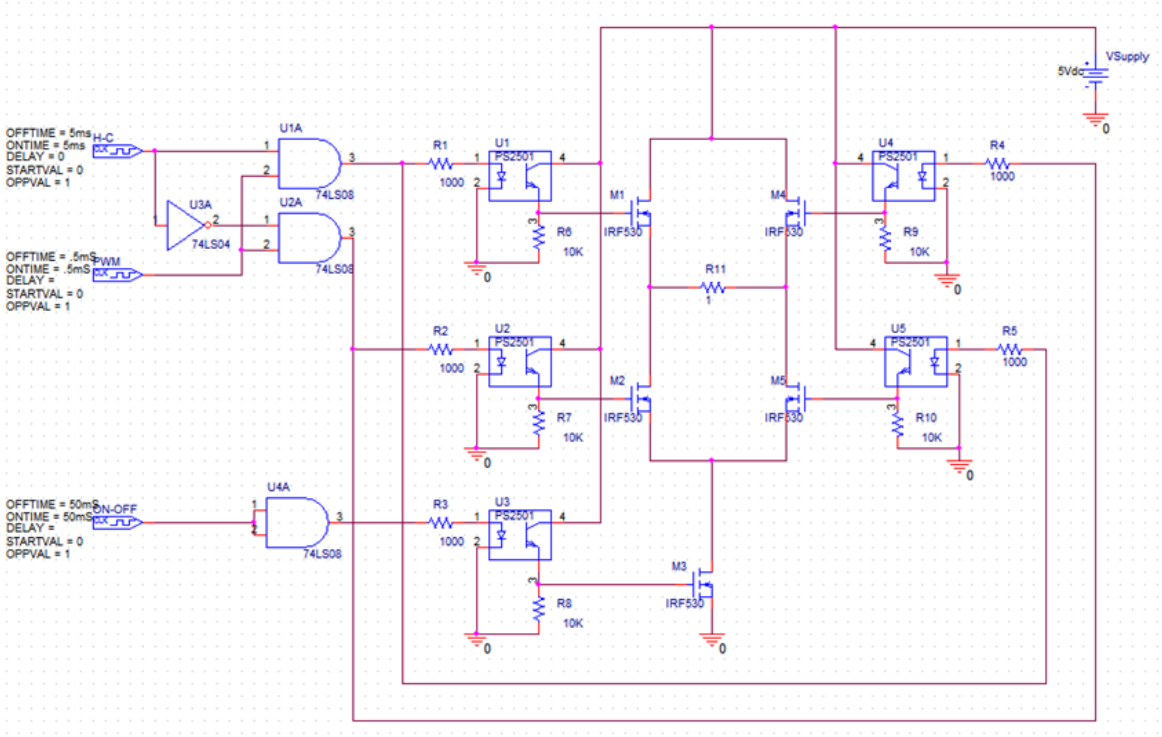

Figure 2.8 The circuit diagram of Peltier control circuit.

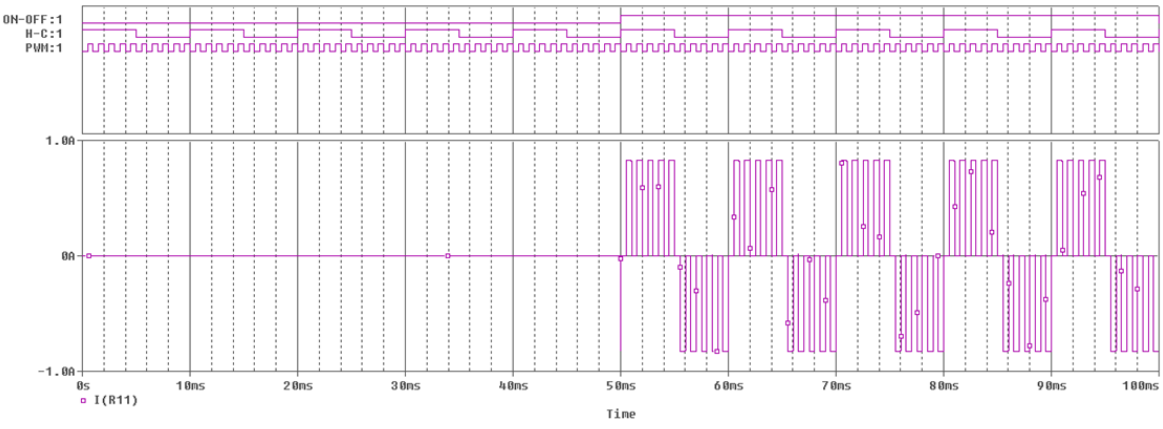

Figure 2.9 The P-Spice simulation of Peltier control circuit.

However, this circuit was burned out because of a huge amount of power consumption. In the second version of the circuit, H-bridge was constructed by replacing MOS transistor and optocoupler structure with relays. In this version, the Peltier is not modulated by PWM.

2.3 LabVIEW based Programming

LabVIEW is a visual programming language developed by National Instruments. There are two pages to design the user interface and the program run behind the interface which are called Block Diagram and Front Panel.

In this study, LabVIEW based user interface was designed to monitor the real time changes in diffuse reflectance and total transmittance. The designed user interface program has a capability

- to save the optical setup parameters and tissue geometry parameters
- to perform and save the measurements to be needed for the normalization
- to monitor and to save the sample temperature
- to decide Peltier working mode (heater or cooler mode)
- to send the data coming from T and R detectors to lock-in amplifier by controlling the analog switch
- to save the reflected and transmitted light information coming out from lock-in amplifier
- to calculate and monitor the normalized reflectance and transmittance
- to prepare the IAD file which is needed to calculate μ_a and μ_s' values

The front panel view of the code is shown in Figure 2.10. The section denoted by A includes the information about experimental setup geometry and sample geometry. The normalization measurements explained in Section 1.4 are performed with the control buttons in the section denoted by B. C section includes the file name, run and stop button and run time indicator. In D section, the initial measurement time adjusts the time required to take measurement in room temperature. The final temperature input determines the final temperature that sample will reach. The temperature indicator and graph help to monitor the temperature changes. There are two led indicators which show the heating or cooling periods. In section E, the normalized transmittance and reflectance values can be monitored.

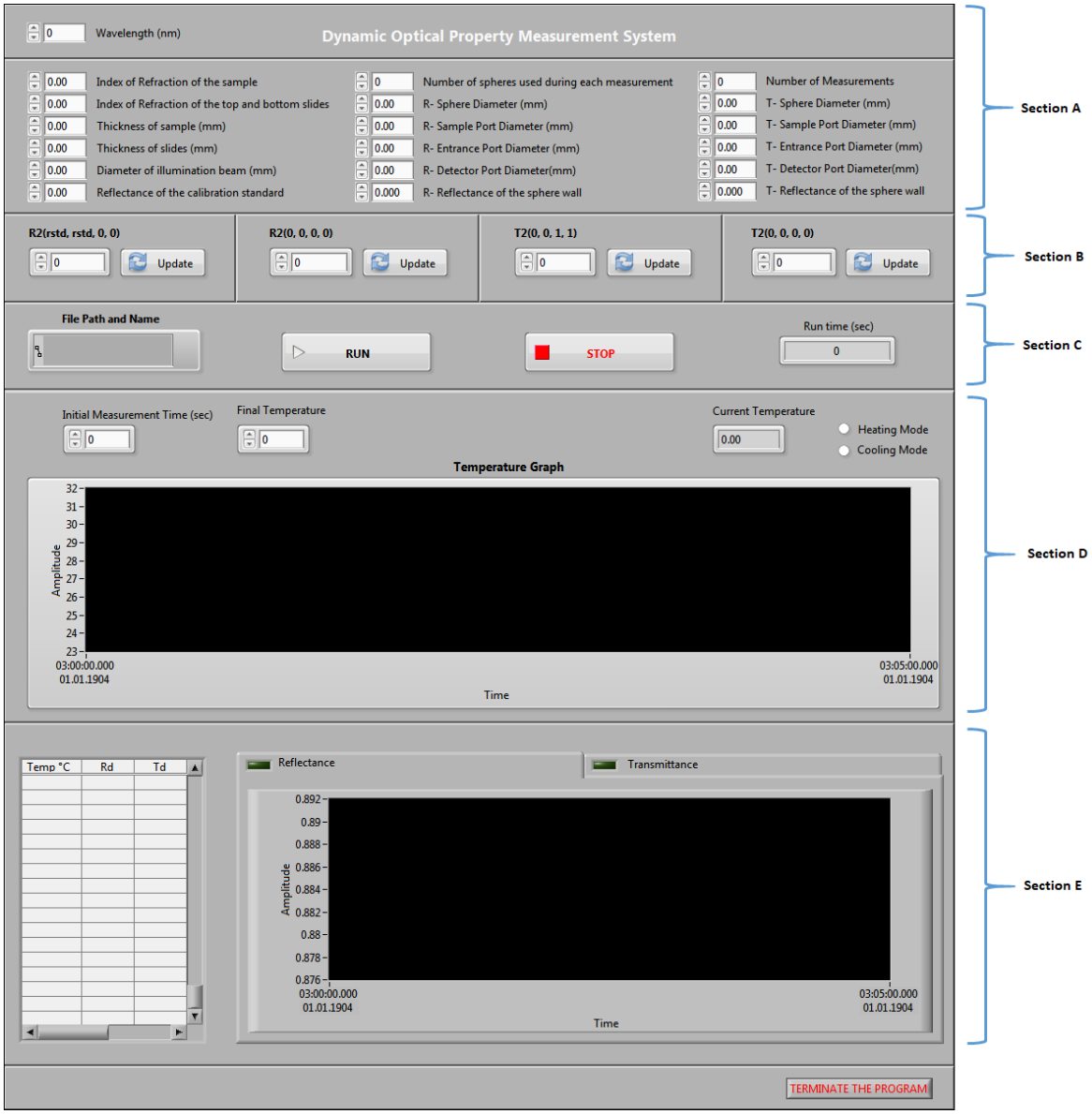

Figure 2.10 User interface.

3. EFFECT OF LIPID CONCENTRATION ON TEMPERATURE RELATED OPTICAL PROPERTIES

In laser applications, optical properties of the tissues should be known before the treatment since they are the prominent factors to determine the interaction of light with the tissue. Tissue type and its lipid content can affect the tissue optical properties. Temperature related changes in optical properties could be different for the same kind of tissues having different lipid content. In order to simulate this effect, the transmittance and reflectance measurements were performed with the lipid emulsions having different lipid concentration. The correlation of transmitted and reflected light with temperature and the effect of lipid concentration were investigated.

3.1 Sample Preparation

OLICLINOMEL N7-1000 with 20% lipid density was used as a lipid emulsion. Oil concentration is 20% olive oil and 80% soybean oil. In the experiments, the emulsion was diluted with a distilled water to prepare five different sample concentrations of 20%, 10%, 5%, 2.5% and 1.25%.

3.2 Experimental Setup

A double integrating sphere system was used to measure the amount of light reflected and transmitted light by the tissue. The system design explained in Section 2 was used. The first version of the control unit was used. The output power of the laser (VA-I-400-635, Optotronics, USA) with a wavelength of 635nm was set at 2mW. LM35 (Texas Instrument) temperature sensor was used. The experimental setup parameters and sample geometry parameters are shown in 3.1.

Table 3.1
Experimental setup and sample parameters.

Parameters	Value
Wavelength (nm)	635
Thickness of sample (mm)	5.5
Diameter of illumination beam (mm)	2.3
Top Slide Thickness (mm)	1.15
Bottom Slide Thickness (mm)	1.15
Reflectance of the calibration standard	0.99
Number of spheres used during each measurement	2
R-Sphere Diameter (mm)	83.8
R-Sample Port Diameter (mm)	12.7
R-Entrance Port Diameter (mm)	12.7
R-Detector Port Diameter (mm)	12.7
R-Reflectance of the sphere wall	0.992
T-Sphere Diameter (mm)	83.8
T-Sample Port Diameter (mm)	12.7
T-Entrance Port Diameter (mm)	25.7
T-Detector Port Diameter (mm)	12.7
T-Reflectance of the sphere wall	0.992

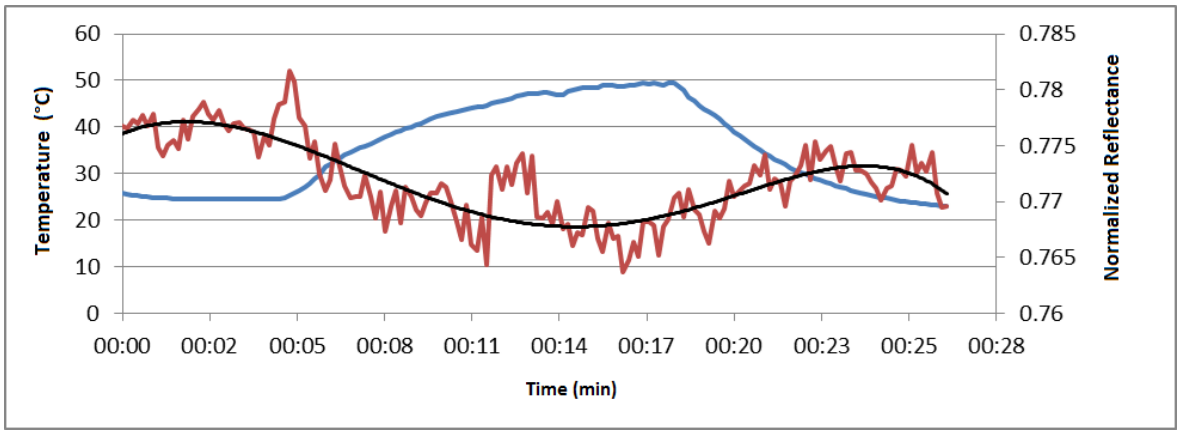

Figure 3.1 Change of normalized reflectance with temperature. The blue line shows temperature, the red line shows the normalized reflectance and the black line shows the fifth order polynomial fitted normalized reflectance.

3.3 Experimental Protocol

After five minutes of measurement at room temperature, the samples were heated to 50°C and were expected to return to room temperature again. The reflected and reflected light values measured at this time were normalized as explained in Section 1.4.

3.4 Results and Discussion

Figure 3.1 and Figure 3.2 show the normalized reflectance-temperature and normalized transmittance-temperature relationships for a 5% lipid emulsion. As the temperature increased, the reflectance decreased but the transmittance increased. Similar behavior was also observed for the other lipid concentrations.

Table 3.2 shows the correlation of the normalized reflectance and transmittance with temperature for different lipid-density emulsions. The correlation coefficients for all reflectance and transmittance values with temperature were statistically significant ($p < 0.05$). As the lipid concentration decreased, the correlation of reflectance with temperature negatively increased. All transmittance measurements showed a positive

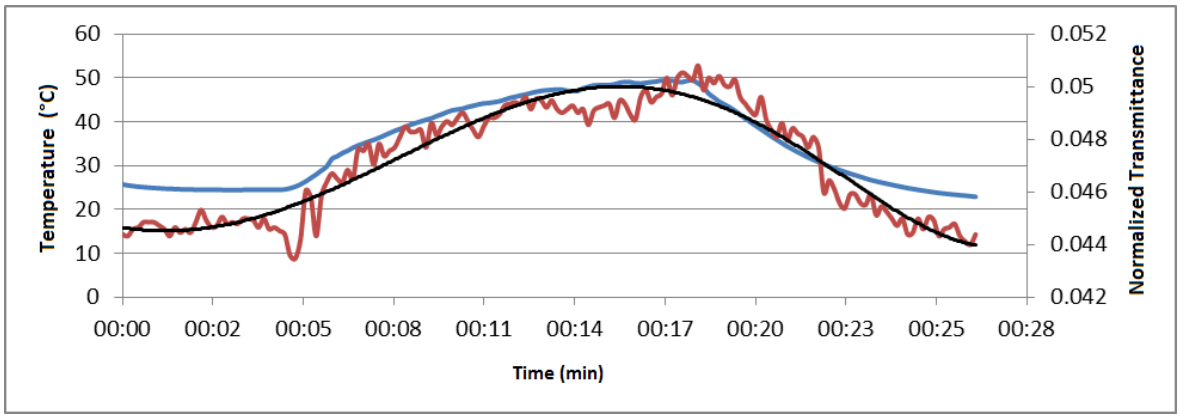

Figure 3.2 Change of normalized transmittance with temperature. The blue line shows temperature, the red line shows the normalized transmittance and the black line shows the fifth order polynomial fitted normalized reflectance.

correlation with temperature. The highest correlation of transmittance with temperature was found at %5 concentrated emulsion as 0.9535.

Figure 3.3 and Figure 3.4 shows the time versus transmittance and reflectance measurements for the all lipid concentrations. It was observed that the normalized reflectance value increased and the normalized transmittance decreased with increasing concentration ratio. It is understood that as the concentration decreases, the light can pass more easily through the sample.

Table 3.2
Correlation coefficient of reflectance and transmittance with temperature for different concentration values.

Concentration Value	Correlation Coefficient	
	Reflectance	Transmittance
20%	-0.1716	0.9285
10%	-0.2484	0.8163
5%	-0.7721	0.9535
2.5%	-0.8594	0.8913
1.25%	-0.8615	0.7880

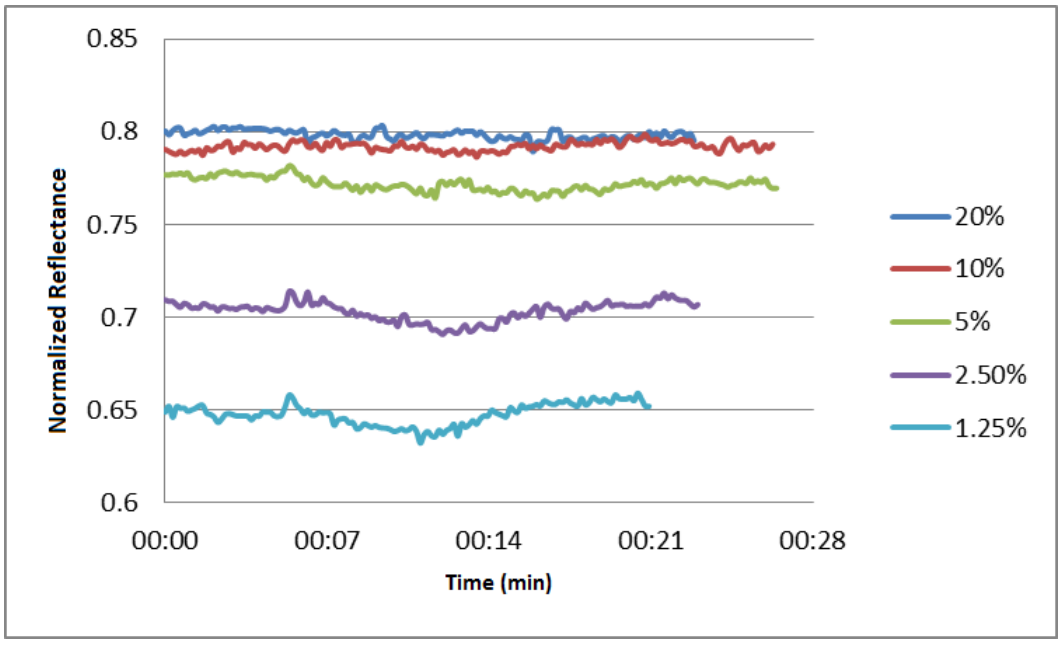

Figure 3.3 Normalized reflectance variations for emulsions having different lipid concentration.

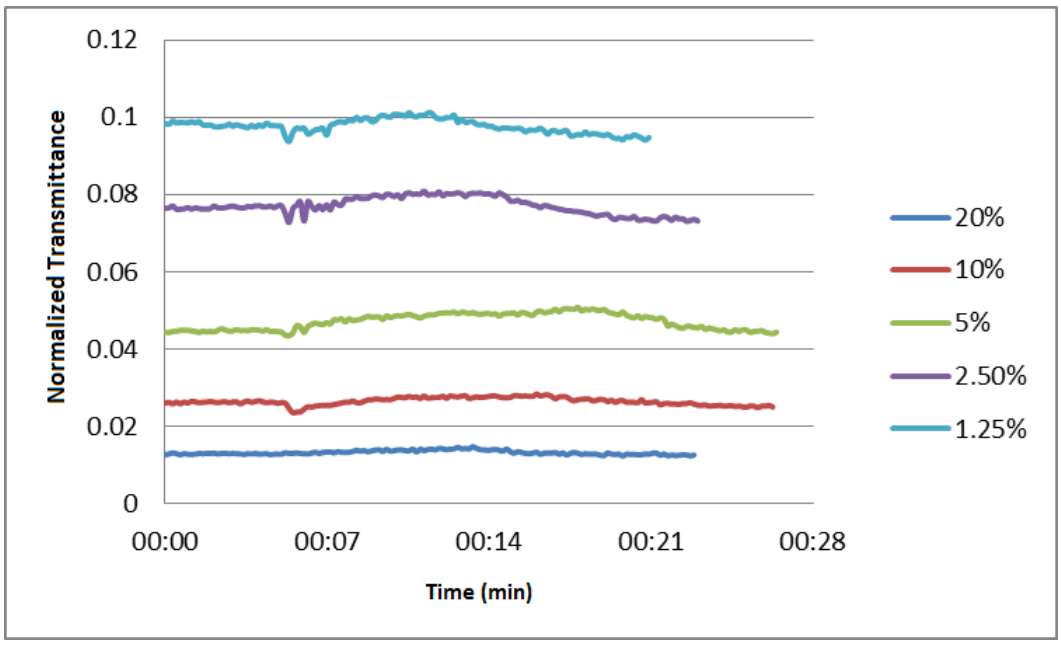

Figure 3.4 Normalized transmittance variations for emulsions having different lipid concentration.

4. EFFECT OF TEMPERATURE ON OPTICAL PROPERTIES OF LIPID EMULSION

Lipid emulsions are generally used to simulate the light interaction mechanisms within the tissue [12, 13, 14, 15, 16, 17, 18, 19]. Such emulsions mainly consist of oil, glycerol, and phospholipid. The absorption spectrum of these emulsions is attributed to water and the scattering is mainly due to scattering particles within the emulsion [12, 17, 18].

In this study, the direct relationship between the optical properties of the lipid emulsion and temperature will be investigated by the designed temperature-controlled system.

4.1 Sample Preparation

OliClinomel is a triple chambered bag parenteral nutrition bag which is consisted of lipid emulsion, amino acid solution and glucose solution. In this study, a 10% lipid emulsion bag of OliClinomel N4-550E (Baxter) was used. The emulsion contains 80% to 20% olive and soybean mixture, egg phosphatide, glycerol, sodium oleate, sodium hydroxide for pH adjustment and water. The content of the emulsion is given in Table 4.1. It was diluted with distilled water to obtain a 2.5% concentrated sample.

4.2 Experimental Setup

A cuvette was prepared by gluing a 2.7-mm-thick acrylic frame and 1-mm-thick glass coverslips. Two ports were opened in the frame to inject the sample into the cuvette and to insert a temperature sensor (LMT84, Texas Instruments). The sample holder design described in Section 2.1 was used. The system design with double-integrating-sphere shown in Figure 2.1 was used. A 635-nm diode laser (VA-I-400-635,

Table 4.1
OliClinomel ingredients.

	OliClinomel N4-550E
Volume	300 ml
Refined Olive Oil + Refined Soy Oil	30 g
Purified Egg Phosphatide	1.80 g
Glycerol	3.38 g
Sodium Oleate	0.05 g
Sodium Hydroxide	qs, pH

Optotronics, USA, 1 mW) was used as the light source. Optical chopper reduced the power to 0.5mW and the irradiance became 0.012W/cm2. The second version of the control unit was used. The setup and sample parameters are listed in Table 4.2.

4.3 Protocol and Optical Property Calculation

The experimental period includes a period of 5-minute measurement at room temperature, a period of heating up to 50°C, and then a period of cooling down to room temperature. Normalized transmittance and normalized reflectance were measured. The reduced scattering and absorption coefficient values were computed by the IAD program. The IAD input parameters were the normalized total transmittance and reflectance, the refractive index of the sample, and the anisotropy factor in addition to the double-integrating-sphere setup and sample parameters.

Glycerin in the sample is dissoluble in water. Oil and phosphatides, also called phospholipids, in glycerin-water solution creates small vesicles that are the main scattering factors of the lipid emulsion [17]. The density of the olive oil, soybean oil and phospholipid are 0.91 g/ml, 0.917 g/ml and 1.097 g/ml, respectively. The refractive index of the lipid emulsion is determined by the formula

Table 4.2
Experimental setup and sample parameters.

Parameters	Value
Wavelength (nm)	635
Index of Refraction of the Sample	1.34
Index of Refraction of the top and bottom slides	1.52
Thickness of sample (mm)	2.7
Top Slide Thickness (mm)	1.0
Bottom Slide Thickness (mm)	1.0
Diameter of illumination beam (mm)	2.3
Number of spheres used during each measurement	2
R-Sphere Diameter (mm)	83.8
R-Sample Port Diameter (mm)	12.7
R-Entrance Port Diameter (mm)	12.7
R-Detector Port Diameter (mm)	12.7
R-Reflectance of the sphere wall	0.992
Number of Measurements	2
T-Sphere Diameter (mm)	83.8
T-Sample Port Diameter (mm)	12.7
T-Entrance Port Diameter (mm)	12.7
T-Detector Port Diameter (mm)	12.7
T-Reflectance of the sphere wall	0.992

$$n_{emulsion} = n_{water} + 0.14\phi_p \tag{4.1}$$

where ϕ_p is the volume concentration of the scattering particles [12, 17, 19]. The refractive index was calculated as 1.34.

It is known that refractive index is dependent on temperature. When temperature rises, the value of refractive index is expected to decreases. Cletus et al. modeled the changes of the refractive index with temperature and found the temperature sensitivity of the refractive index of intralipid as -3.54x10$^{-4}K^{-1}$ [16]. In our study, temperature varied about 30°C. The refractive index change due to temperature variation would be 0.01. We assume that it is negligible for this temperature range.

Also, the anisotropy factor was calculated by

$$g = 1.1 - 0.58\lambda \tag{4.2}$$

where λ is wavelength in micrometers[17]. g was calculated as 0.73.

Multi Layered Monte Carlo simulation program developed by L. Wang and S. L. Jacques was used to observe the effect of optical property changes due to temperature on the light propagation. The obtained scattering and absorption coefficients at 21°C and 50°C were used to calculate the corresponding fluence rates by using one million photons.

4.4 Results and Discussion

Temperature dependence of the reflectance and transmittance of a 2.5% concentrated lipid emulsion is presented in Figure 4.1. The normalized diffuse reflectance

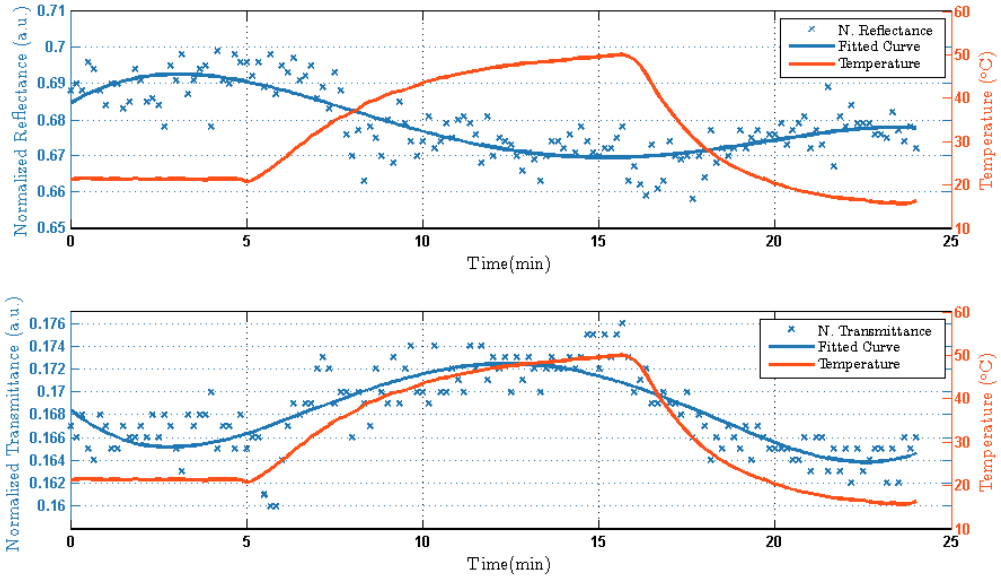

Figure 4.1 Normalized transmittance, normalized reflectance, and temperature measurements as functions of time.

and total transmittance data are indicated by blue stars. The blue and orange lines show the fourth-order polynomial fitted to the data and the sample temperature over time, respectively. The reflectance showed a negative correlation and the transmittance showed a positive correlation with temperature. The correlation coefficients for transmittance and reflectance were found to be 0.8586 and -0.4896, respectively. They are statistically significant for both cases. It may be speculated that the volume variations of the sample due to the temperature change have an effect on the reflection and transmittance behaviors.

Figure 4.2 shows the temperature-dependent absorption and reduced scattering coefficients of 2.5% lipid emulsion. As in the previous figure, the normalized diffuse reflectance and total transmittance data are denoted by blue stars. The blue and orange lines show the fourth-order polynomial fitted to the data and the sample temperature over time, respectively. The correlation coefficient between the absorption coefficient and temperature is 0.0633 but it is not statistically significant ($p \geq 0.05$). The absorption characteristics of lipid emulsion is attributed to water spectrum. However, the absorption of water and its temperature dependence at 635nm is very low[20, 21, 22].

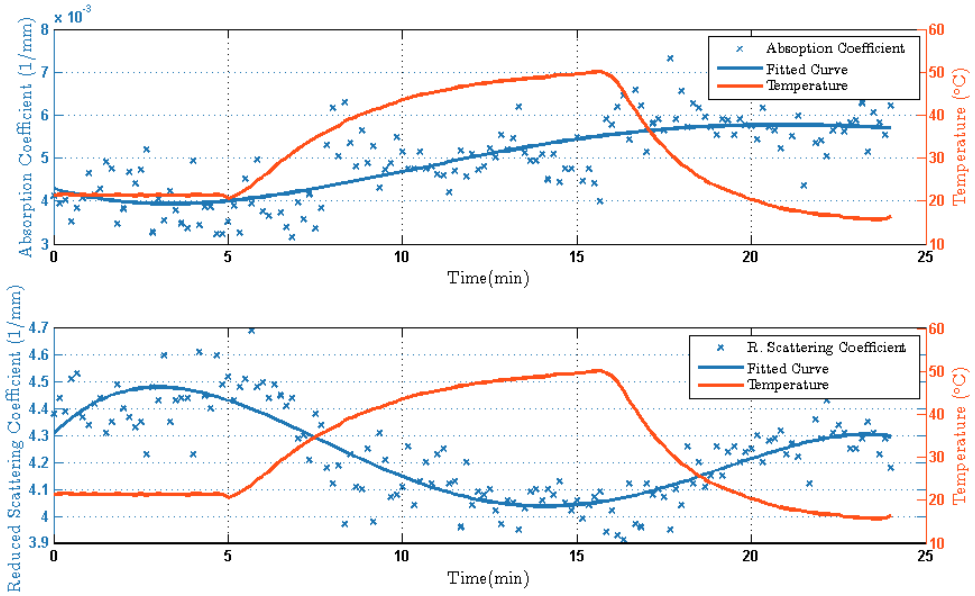

Figure 4.2 Absorption coefficients, reduced scattering coefficients, and temperature as functions of time.

This could explain the low correlation coefficient and low statistic.

The reduced scattering coefficient showed a statistically significant negative correlation of -0.7039 with temperature. Egg phospholipid in the emulsion forms small vesicles having monolayer and bilayer membranes[17]. The number and geometry of these small vesicles in lipid emulsion are the main factor affect the scattering coefficient. The sample volume increases with increasing temperature and the number scattering particles per volume decreases. This might result in a decrease in the scattering coefficient.

The change in lipid emulsion could be irreversible because the values of both the absorption and reduced scattering coefficients are different after the sample heated. Cletus et al. found that the absorption coefficient at 840 nm was higher and the reduced scattering coefficient at 740 nm was lower during the cooling period than heating period [16]. We observed these effects for both the absorption and scattering coefficients at 635 nm. It can be concluded the physical structure of lipid might be changed due to temperature.

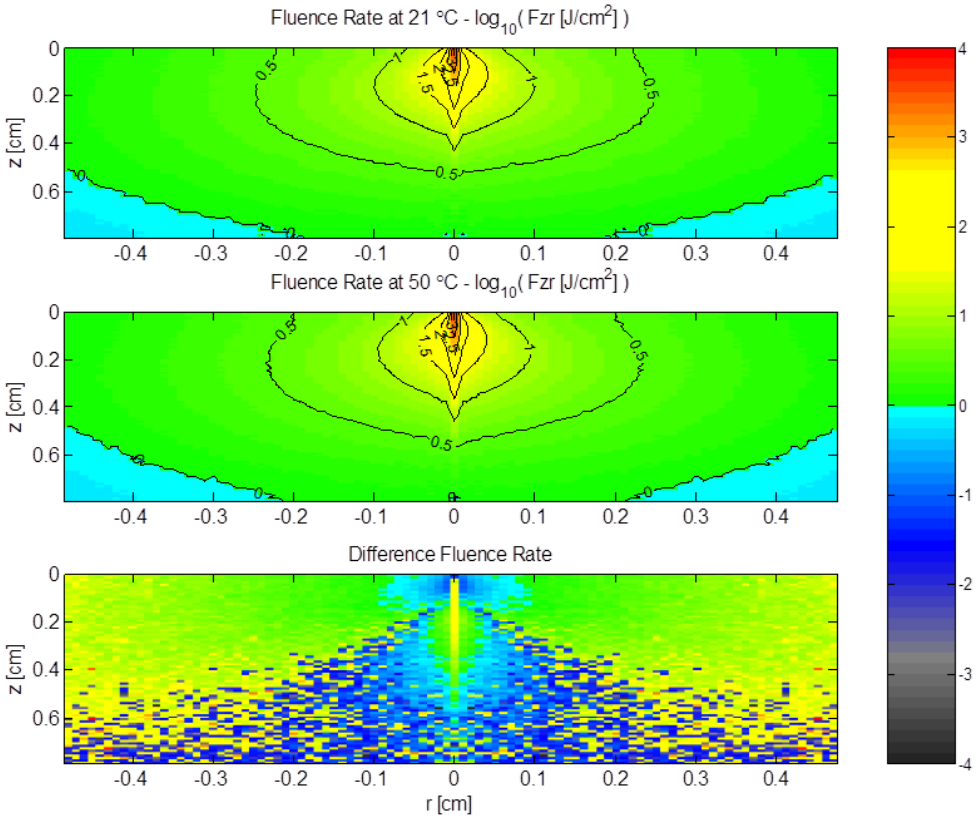

Figure 4.3 Monte Carlo simulation results: (a) fluence rate at 21°C, (b) fluence rate at 50°C, and (c) difference in the fluence rates between 21°C and 50°C.

In order to observe the effect of temperature on light propagation, we performed a Monte Carlo simulation by using the absorption and the scattering coefficients obtained previously at 21°C and 50°C. The fluence rates at these two temperatures and the difference in logarithmic scale are shown in Figure 4.3. The positive colors show that the fluence rate at 50°C is higher than that at 21°C. Alterations in the fluence rate was observed and it showed that the optical property changes due to temperature can change the fluence rate and the light propagation within the tissue.

5. CONCLUSION

In this thesis, a new optical measurement system with a heating-cooling mechanism was designed to monitor temperature-dependent optical property measurements using a double-integrating sphere. The studies having a double integrating sphere setup to measure temperature dependent optical properties can be categorized into three groups. The first group contains the water bath connected sample holder designs [7, 9]. The hot water is pumped from the hot water bath through a custom made sample holder. It can be difficult to change the temperature quickly with such designs. Also, it can be quite troublesome to set up a water-controlled system next to the optical system. The second group contains temperature controlled boxes [8, 11]. In addition to the difficulty of installing optical setup in a closed box, integrating spheres and detectors will be heated together with sample. Although the coating material of integrating spheres has a low temperature sensitivity, heating of detectors will cause an increase in the noise at detectors. The last group includes the designs with hot plates [10]. The size restrictions of the hot plate make it difficult to perform the optical measurements with double integrating sphere because there is no enough space to put it between two spheres. The sample holder design with Peltier allows us to realize a compact sample holder with no moving parts and no circulating fluids.

The system was tested with a lipid emulsion which is generally used as an optical tissue-mimicking phantom in literature. The absorption coefficient showed a positive correlation whereas the scattering coefficient showed a positive correlation with temperature. The obtained results imply that temperature variations can change the optical properties and it may be due to the physical changes of the scattering particles. Also, Monte Carlo simulation showed that the variations in the coefficients change the light propagation within the tissue. Therefore, temperature-dependent dynamic changes especially in tissues having high lipid content should be taken into consideration for a safe laser treatment.

The direct relationship between optical properties and temperature were investigated by the designed experimental setup. The optical properties of the sample were measured by increasing and decreasing the temperature. As a future work, the sample can be heated to a high constant temperature and how the optical properties change over time could be observed under the constant temperature. Also, lipids may undergo the phase transitions when its temperature increases. The effect of the phase transitions on the lipid optical properties may be investigated with this system.

6. List of publications produced from the thesis

1. Sıcaklığın Oliclinomelin Optik Özellikleri Üzerine Etkisi, E. Kara, M. Gülsoy, *18th National Biomedical Engineering Meeting*, Istanbul, 2014.

2. Monitoring System for Investigating the Effect of Temperature Change on Optical Properties E. Kara, İ. Çilesiz, M. Gülsoy *Lasers in Medical Science*, 2018, doi:10.1007/s10103-018-2537-2.

REFERENCES

1. Niemz, M. H., *Laser-Tissue Interactions*, Biological and Medical Physics, Biomedical Engineering, Berlin, Heidelberg: Springer Berlin Heidelberg, 2007.

2. Sviridov, A. P., and A. V. Kondyurin, "Optical characteristics of cartilage at a wavelength of 1560 nm and their dynamic behavior under laser heating conditions.," *Journal of Biomedical Optics*, Vol. 15, no. 5, p. 055003, 2011.

3. Welch, A. J., and M. J. van Gemert, eds., *Optical-Thermal Response of Laser-Irradiated Tissue*, Dordrecht: Springer Netherlands, 2011.

4. Prahl, S. A., M. J. C. van Gemert, and A. J. Welch, "Determining the optical properties of turbid media by using the adding doubling method," *Applied Optics*, Vol. 32, p. 559, feb 1993.

5. Morales Cruzado, B., S. V. y Montiel, and J. A. D. Atencio, "Genetic algorithms and MCML program for recovery of optical properties of homogeneous turbid media," *Biomedical Optics Express*, Vol. 4, p. 433, mar 2013.

6. Prahl, S. A., "Everything I think you should know about Inverse Adding-Doubling." Available: https://omlc.org/software/iad/manual.pdf.

7. Agah, R., A. Gandjbakhche, M. Motamedi, R. Nossal, and R. Bonner, "Dynamics of temperature dependent optical properties of tissue: dependence on thermally induced alteration," *IEEE Transactions on Biomedical Engineering*, Vol. 43, pp. 839–846, aug 1996.

8. Laufer, J., R. Simpson, M. Kohl, M. Essenpreis, and M. Cope, "Effect of temperature on the optical properties of ex vivo human dermis and subdermis.," *Physics in Medicine and Biology*, Vol. 43, pp. 2479–89, sep 1998.

9. Skinner, M. G., S. Everts, A. D. Reid, I. A. Vitkin, L. Lilge, and M. D. Sherar, "Changes in optical properties of ex vivo rat prostate due to heating," *Physics in Medicine and Biology*, Vol. 45, pp. 1375–1386, may 2000.

10. Basu, R., S. H. Diaz-Valdes, B. J. Wong, and S. J. Madsen, "Temperature- and wavelength-dependent scattering of light during slow heating of porcine septal cartilage," in *Proc. SPIE 4617, Laser Tissue Interaction XIII: Photochemical, Photothermal, and Photomechanical* (Jacques, S. L., D. D. Duncan, S. J. Kirkpatrick, and A. Kriete, eds.), Vol. 4617, pp. 67–76, jun 2002.

11. Kim, S., and S. Jeong, "Effects of temperature-dependent optical properties on the fluence rate and temperature of biological tissue during low-level laser therapy," *Lasers in Medical Science*, Vol. 29, pp. 637–644, mar 2014.

12. Michels, R., F. Foschum, and A. Kienle, "Optical properties of fat emulsions," *Optics Express*, Vol. 16, p. 5907, apr 2008.

13. Ninni, P. D., F. Martelli, and G. Zaccanti, "Intralipid: towards a diffusive reference standard for optical tissue phantoms.," *Physics in Medicine and Biology*, Vol. 56, no. 2, pp. N21–N28, 2011.

14. McGlone, V. A., P. Martinsen, R. Künnemeyer, B. Jordan, and B. Cletus, "Measuring optical temperature coefficients of Intralipid®," *Physics in Medicine and Biology*, Vol. 52, pp. 2367–2378, May 2007.

15. Solarte, E., "Lipid Concentration Effects on Light Propagation in Liquid Phantoms," in *Biomedical Optics 2014*, (Washington, D.C.), p. BS3A.31, OSA, 2014.

16. Cletus, B., R. KuÌnnemeyer, P. Martinsen, and V. A. McGlone, "Temperature-dependent optical properties of Intralipid® measured with frequency-domain photon-migration spectroscopy," *Journal of Biomedical Optics*, Vol. 15, no. 1, p. 017003, 2010.

17. van Staveren, H. J., C. J. Moes, J. van Marie, S. a. Prahl, and M. J. van Gemert, "Light scattering in Intralipid-10% in the wavelength range of 400-1100 nm.," *Applied Optics*, Vol. 30, no. 31, pp. 4507–4514, 1991.

18. Flock, S. T., S. L. Jacques, B. C. Wilson, W. M. Star, and M. J. C. van Gemert, "Optical properties of intralipid: A phantom medium for light propagation studies," *Lasers in Surgery and Medicine*, Vol. 12, no. 5, pp. 510–519, 1992.

19. Aernouts, B., R. V. Beers, R. Watté, and J. Lammertyn, "Dependent scattering in Intralipid ® phantoms in the 600-1850 nm range," *Optics Express*, Vol. 22, no. 5, pp. 993–996, 2014.

20. Langford, V. S., A. J. McKinley, and T. I. Quickenden, "Temperature dependence of the visible-near-infrared absorption spectrum of liquid water," *The Journal of Physical Chemistry A*, Vol. 105, no. 39, pp. 8916–8921, 2001.

21. Buiteveld H, Hakvoort JHM, D. M., "Optical properties of pure water," in *In: Jaffe JS (ed) SPIE Ocean Opt. XII.*, pp. 174–183, 1994.

22. Pegau WS, Z. J. V., "Temperature dependence of the absorption coefficient of pure water in the visible portion of the spectrum," in *In: Jaffe JS (ed) Proc. SPIE 2258, Ocean Opt. XII.*, pp. 597–604, 1994.